Tectonophysics 602 (2013) 69–77

Contents lists available at SciVerse ScienceDirect

Tectonophysics

journal homepage: www.elsevier.com/locate/tecto

The thermal structure of Israel and the Dead Sea Fault

Eyal Shalev [a,*], Vladimir Lyakhovsky [a], Yishai Weinstein [b], Zvi Ben-Avraham [c]

[a] Geological Survey of Israel, 30 Malkhe Israel, Jerusalem, 95501, Israel
[b] Department of Geography and Environment, Bar-Ilan University, Ramat-Gan, 52900, Israel
[c] Department of Geophysics and Planetary Sciences, Tel-Aviv University, Tel-Aviv 69978, Israel

ARTICLE INFO

Article history:
Received 1 November 2011
Received in revised form 28 August 2012
Accepted 13 September 2012
Available online 23 September 2012

Keywords:
Heat flux
Seismogenic zone
Thermal structure
Dead Sea Fault

ABSTRACT

In this paper we analyze temperature data from all the available oil and water wells in Israel and compare the results with seismicity depth and with heat flux estimation from xenoliths. We show that the average heat flux in Israel is 40–45 mW/m^2, consistent with measurements of the Arabian Shield. A heat flux anomaly exists in Northern Israel and Jordan. This could be attributed to groundwater flow or young magmatic activity (~100,000 years) that is common in this area. A higher heat flux exists in Southern Israel and Jordan, probably reflecting the opening of the Red Sea and the Gulf of Eilat (Gulf of Aqaba) and does not represent the average value present in the Arabian Shield.

The temperature gradient at the Dead Sea basin is relatively low, resulting in low heat flux (<40 mW/m^2) and a relatively deep seismicity extending to lower crustal depths, in agreement with earthquake depths (<25–30 km). Higher heat fluxes at the Sea of Galilee (70 mW/m^2) and at the Gulf of Eilat (65 mW/m^2) results with shallower seismicity (<10–12 km). The steep geothermal gradients yielded by xenoliths (>80 mW/m^2) could be the result of local heating by magmas or by lithospheric necking and shear heating.

1. Introduction

Heat flux is a major factor that affects the rheology of the lithosphere, magmatism, and groundwater flow (Ranalli and Rybach, 2005). Different assumptions about the heat flux in Israel have led to different tectonic and seismological models (Aldersons et al., 2003; Al-Zoubi and ten Brink, 2002; Sobolev et al., 2005). The heat flux controls the thickness of the lithosphere, the type of deformation (brittle versus ductile), and the depth of the seismogenic zone (Jaupart and Mareschal, 2011; Ranalli, 1995). Sobolev et al. (2005) and Petrunin and Sobolev (2006) presented results of a three-dimensional thermomechanical model of a pull-apart basin, formed at left stepping segments of an active continental transform fault such as the Dead Sea (see Fig. 1 for location). Adopting the classical scheme of a pull-apart basin formation, they demonstrated that the major parameter controlling the basin structure and deformation pattern beneath the basin is the thickness of the brittle layer. Significant ductile deformation of the lower crust and the upper mantle associated with basin growth due to a pull-apart mechanism requires normal or elevated heat flux. The closest fit to the Dead Sea structure has been obtained with the model corresponding to a surface heat flow above 60 mW/m^2. They also argued that a strong lower crust in a cold lithosphere with heat flow below 50 mW/m^2 could not allow the opening of a pull-apart such as the Dead Sea basin.

Förster et al. (2007) determined the heat flux in five, up to 900 m deep boreholes in southern Jordan to be 60.3 mW/m^2. Recently, Förster et al. (2010) analyzed a set of surface samples from the uppermost crust down to the lithospheric mantle underneath Jordan and assumed heat flux of 55–65 mW/m^2 to construct a thermal model. Thermobarometric calculations, based on lower crustal and lithospheric mantle xenoliths, suggest even steeper geothermal gradients (e.g. Al-Mishwat and Nasir, 2004; McGuire, 1988; McGuire and Bohannon, 1989; Nasir, 1992; Stein et al., 1993), thus higher heat flux (>80 mW/m^2). The above considerations contradict the general view of the Arabian Shield as an anomalously cold terrain characterized by heat flux values below ~45 mW/m^2 (Gettings and Showail, 1982). Davies and Davies (2010) showed that the heat flux along the Red Sea is very high (>150 mW/m^2), whereas the heat flux at the Arabian Shield is low (<55 mW/m^2). Measurements supporting low geothermal heat flux were published by Eckstein (1976), Eckstein and Simmons (1978), Levitte et al. (1984), and Eckstein and Maurath (1995) who measured thermal gradients and thermal conductivity in abandoned oil wells and unused water boreholes distributed over Israel. They calculated an average heat flux of 42 mW/m^2. The mean value of the corrected heat data for the northern part of the Dead Sea basin is 38 mW/m^2 (Ben-Avraham et al., 1978). Recent re-evaluation of the heat flow data for the Dead Sea basin (Shalev et al., 2007) confirmed these low values. Based on coal rank measurements, Bein and Feinstein (1988) showed that a low heat flux has prevailed in the Dead Sea area since the mid-Miocene period. Galanis et al. (1986) estimated a mean basal heat-flow value of 53 mW/m^2 in Jordan. Local elevated heat flux

* Corresponding author. Tel.: +972 50 6234890.
E-mail address: eyal@gsi.gov.il (E. Shalev).

0040-1951/$ – see front matter
http://dx.doi.org/10.1016/j.tecto.2012.09.011

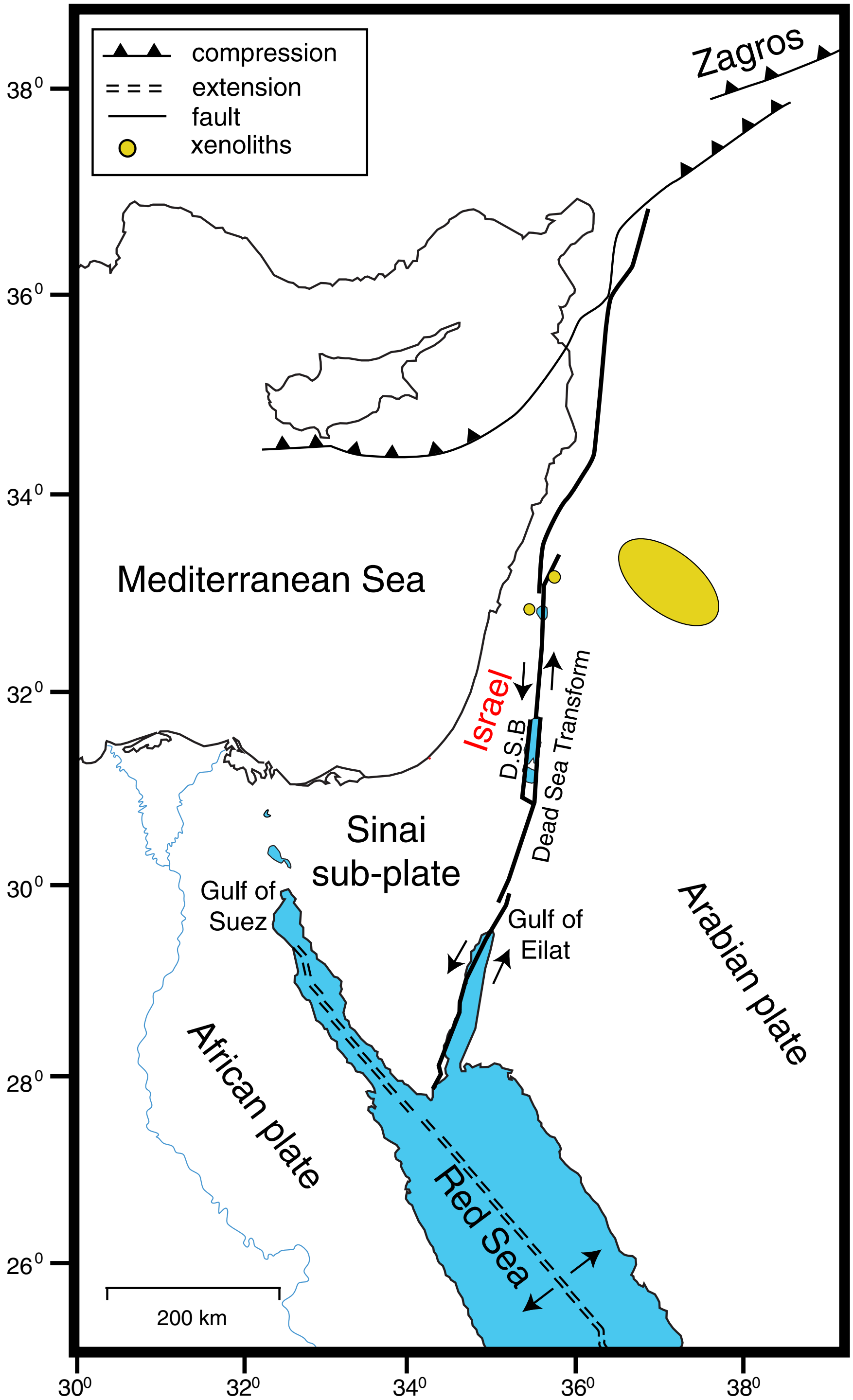

Fig. 1. Major tectonic features of the study area (Israel) and vicinity. The Dead Sea Basin (D.S.B.) is located at the center of the Dead Sea Transform.

values were shown to be associated with groundwater advection (Galanis et al., 1986; Gvirtzman et al., 1997; Kovach et al., 1990; Truesdell et al., 1983).

Another characteristic of the Dead Sea fault is the significant variations in the depth of the seismogenic zone. In the central part (the Dead Sea basin) the seismicity is anomalously deep extending almost to the mantle (Aldersons et al., 2003; Braeuer et al., 2010; Shamir, 2006). Sixty percent of well-constrained micro-earthquakes ($ML \leq 3.2$) in the Dead Sea basin during the period 1984–1997 were located at depths up to 25–30 km. The seismogenic zone becomes shallower to the south, toward the Gulf of Eilat, where most earthquakes are located at depths shallower than 10 km (the European-Mediterranean Seismological Centre catalog, 2011). Recent study of the seismicity in the northern part of the Dead Sea fault (Navon, 2011) shows that at the Sea of Galilee area, the seismogenic zone is also shallow (~12 km) and that it deepens northwards.

The two opposing opinions of high versus low heat flux suffer from some limitations. The analysis of Förster et al. (2007) is based on a very detailed study of just five closely located boreholes in southern Jordan, which they extrapolated on the entire region. On the other hand, the analysis of Eckstein and Simmons (1978), which suggested low heat flux, does not include many new measurements that were collected in recent years.

The purpose of this paper is to re-examine the geothermal heat data collected in Israel for the past 50 years and to determine the average geothermal heat flux in this area. Subsequently, we compare the depth of the seismogenic zone along the Dead Sea Fault with the depth of the isotherm corresponding to the brittle–ductile transition.

2. Geological setting

The crust of the Arabian Shield is composed of Phanerozoic sedimentary rocks overlying a Late Proterozoic crystalline basement (Garfunkel, 1988; Ginzburg and Gvirtzman, 1979). The basement consists of metamorphic and plutonic rocks (mainly granite and diorite compositions). In Israel, these old rocks (older than 550 Ma) are exposed only in the Eilat area and are covered by thick sedimentary sequences throughout most of Israel (Fig. 2). The sedimentary cover thickens toward the northwest and consists mainly of limestone and dolomite, as well as minor chalk, sandstone, clay and evaporites (Rybakov and Segev, 2004).

The tectonic activity along the Red Sea was accompanied by widespread volcanism since the Oligocene, mainly on its Arabian side. Northern Israel is the only place, where extensive volcanism is also found on the Sinai sub-plate. Volcanism is intra-plate, alkali–basaltic in nature (e.g. Weinstein et al., 2006), composed mainly of basaltic flows and scoria cones. It mainly occurs in northern Israel, with thicknesses

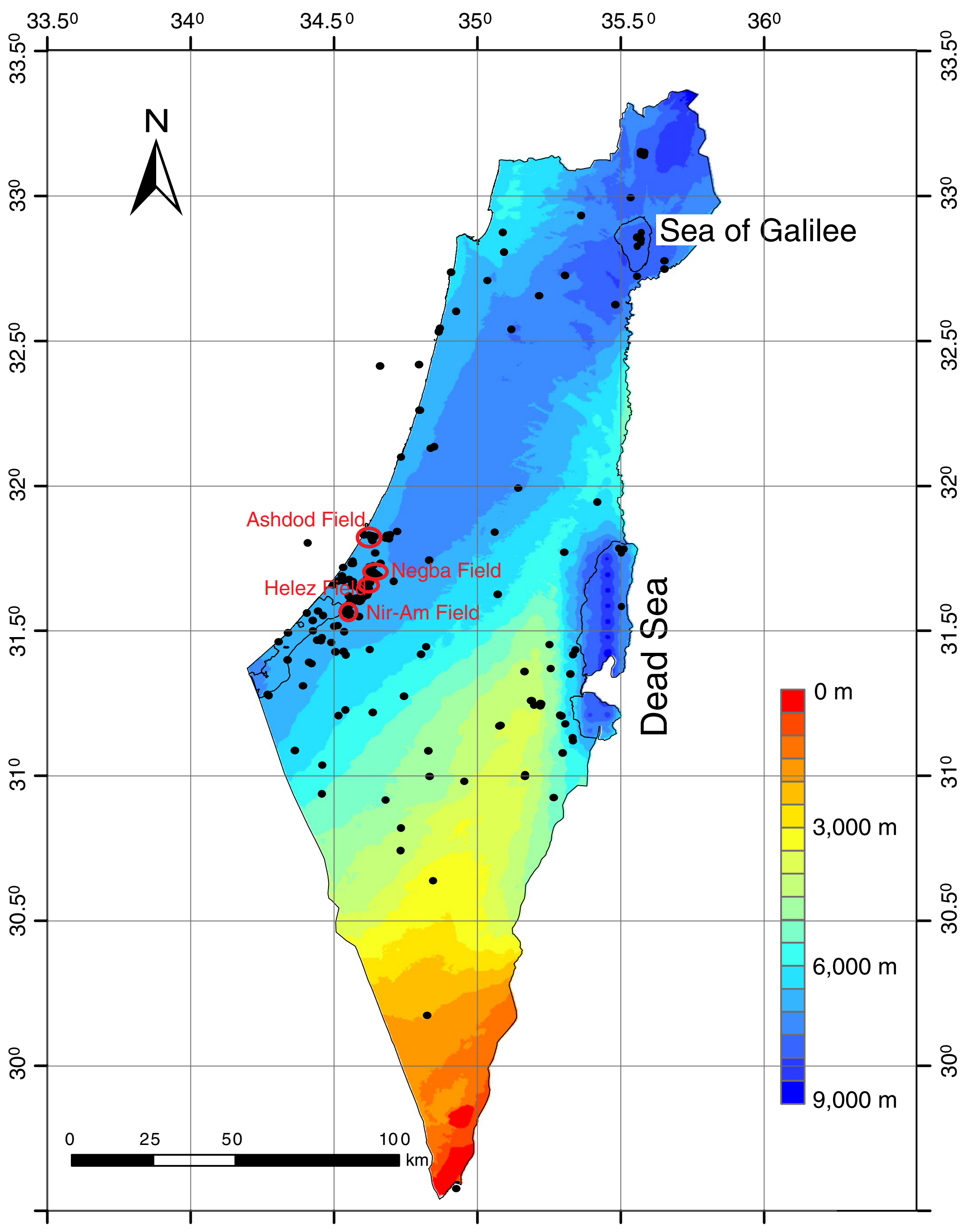

Fig. 2. The depth of the crystalline basement from the surface (after Rybakov and Segev, 2004; Segev et al., 2006). This depth represents the sediment thickness. In southern Israel the basement is exposed. The boreholes from which data was taken are marked by black dots.

between a few tens of meters and more than 800 m. Volcanism in this area is Middle Miocene (17 Ma; Shaliv, 1991) to Late Pleistocene (100 Ka, e.g. Mor, 1993; Weinstein et al., 2009; Shaanan et al., 2010), but younger ages (a few thousand years) were reported for some nearby Syrian basalts (Dubertret, 1954).

The tectonic regime of Israel has considerably changed at ~15 Ma ago with the opening of the Red Sea and Gulf of Eilat. A new regional plate boundary was formed along the sinistral Dead Sea strike-slip fault system, which separates the Sinai sub-plate from the Arabian plate (Fig. 1). Since the formation of the Dead Sea transform, the Arabian plate has been displaced by ~105 km northwards relative to the Sinai sub-plate. Smit et al. (2010) argued that initially deformation of the Dead Sea Fault was pure strike-slip, followed by a second stage with addition of a minor transtensional component. Several deep basins developed along the Dead Sea Fault: Gulf of Eilat, Dead Sea, Sea of Galilee, and Hula Valley (Smit et al., 2008a). These basins are topographically low and their sedimentary cover is very thick. At the Dead Sea basin, the thick salt layer (>2 km) of the Sedom formation has been rising to form many diapirs (Smit et al., 2008b). Farther south, the Arabian plate is diverging from the African plate while creating and widening the Red Sea. The different tectonic setting of the Red Sea Rift (extension) and the Dead Sea Fault (shear) have implications on the heat flux along these fault systems (high along the Red Sea and low along the Dead Sea Fault).

3. Temperature data

Temperature was measured by three major methods: temperature logging, drill stem test, and bottom-hole temperature. Most of the data was published by Shalev et al. (2008).

3.1. Temperature logging

Logs of continuous temperature measurements were taken in several oil and water wells in Israel with the precision of ±0.001 °C. These measurements, when done years after drilling, are considered to provide the most reliable data, representing the true formation temperature (the temperature of the geological formation). On the other hand, temperature logs taken during and close after drilling do not represent the true temperature. This is because during drilling, cement is often used to plug various intervals and it generates considerable heat while setting. Therefore, these logs and are ignored in this study.

3.2. Drill Stem Test (DST)

Drill Stem Test (DST) is a procedure used to determine the productive capacity, pressure, permeability or extent of an oil or gas reservoir. DST is usually conducted with a downhole shut-in tool that allows the well to be opened and closed at the bottom of the hole or above the screen with a surface-actuated valve. Temperature is often measured during the test. These temperature measurements are considered to be a reliable formation temperature when the test has recovered a fair amount of formation water.

3.3. Bottom-Hole Temperature (BHT)

Bottom-hole temperature (BHT) is the temperature in the borehole at total depth at the time it is measured. BHT data are routinely obtained during wire-line logging operations and are taken as the maximum recorded temperature during a logging run. The temperatures are typically lower than the true virgin formation rock temperature due to the cooling effect of the drill fluid circulation. If a bottom-hole temperature can be measured several times at a fixed depth while the well is shut in (no drill fluid circulation), it is possible to monitor the well bore temperature as it recovers toward its pre-drilling state, thus permitting extrapolation to virgin rock temperature. However, in the oil wells in Israel, BHT was not measured in every logging operation. In many cases, the temperature from one logging run was copied later to another log. Therefore, every depth has only one record of measured temperature.

3.4. Calculated temperature-depth data base

Förster (2001) showed that in the German basin, temperatures perturbed by drilling and mud circulation are higher than the true formation temperature at shallow depth and, below the pivot point, they are lower. In this study, we used the Harrison et al. (1983) correction that was developed for North American data, which relates the difference between the formation temperature and BHT to the depth (Z) at which it is measured:

$$T_{cor} = -16.51 + 1.83{*}10^{-2}{*}Z - 2.34{*}10^{-6}{*}Z^2. \tag{1}$$

The T_{cor} values are added to the original BHT values. Z is the depth in meters. The equation is similar to the ones originally proposed by Kehle et al. (1970) and was applied to produce geothermal maps for North America (Blackwell and Richards, 2004a,b; Blackwell et al., 2007; Tester et al., 2006).

Fig. 3 shows that the newly corrected BHT closely fits with DST data and is in a good agreement with the temperature log for the Helez field (Fig. 3d), supporting the correction of Eq. (1). These corrected values are used below for calculating temperature at depth and heat flux maps. In this analysis, only wells that have temperatures measured at more than three different depths are included (altogether, 221 wells).

4. Data interpolation

A geothermal gradient was calculated for each well with reliable newly generated temperature data. The temperature distribution in the homogeneous layer with the thermal conductivity, K_1 and the radiogenic heat production H_1 was calculated using the analytical solution of the equation for the heat transfer which has a parabolic form:

$$T(z) = T_0 + z(q_s/K_1) - z^2 H_1/(2K_1) \tag{2}$$

where z is the depth beneath the surface, T_0 is the temperature at the surface, q_s is the surface heat flux. The thermal conductivity was estimated for each well based on its lithology (Table 1). We assigned the whole Mesozoic and older sedimentary sequence that consists mainly of dolomite, limestone and sandstone a radiogenic heat production of 0.7 $\mu W/m^3$. Younger sediments that consist mainly of chalk, shales, and clay were assigned a radiogenic heat production of 1 $\mu W/m^3$. Upper crust, basement rocks and lower crust were assigned values of 1 $\mu W/m^3$ and 0.2 $\mu W/m^3$, respectively. The surface heat flux, q_s was estimated for every borehole using the best fit between measured values and values calculated using Eq. (2). We note here that some uncertainty in the radiogenic heat production H_1 has a very minor effect on the estimated value of the surface heat flux which is shown in Fig. 4.

It is apparent from Fig. 4 that in most of the studied area, the heat flux is between 35 and 55 mW/m^2. Higher values were found only southeast of the Sea of Galilee (up to ~90 mW/m^2) and in the southernmost part of Israel, with values close to the Gulf of Eilat approaching 80 mW/m^2. Few very low measurements (<30 mW/m^2) were recorded at the deep basin of the Dead Sea and in northwestern Israel. Such exceptionally low values were measured in some deep basins such as the Gulf of Mexico and the Great Basin, California (Blackwell et al., 2007).

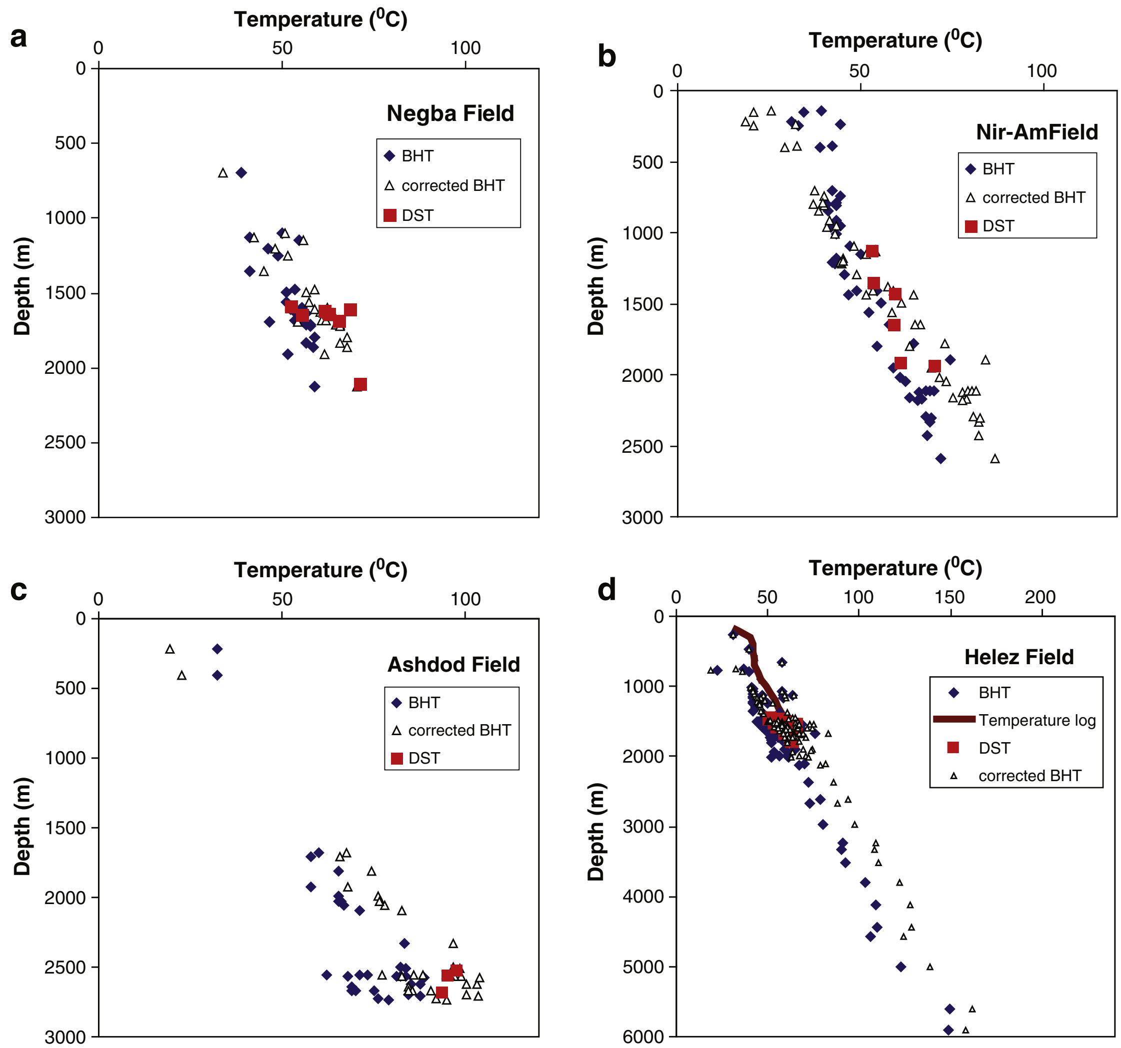

Fig. 3. Measured and corrected bottom-hole temperature (BHT) along with measured drill stem temperature (DST) and temperature logs. a. Negba, b. Nir-Am, c. Ashdod, and d. Helez fields (see Fig. 2 for location).

Temperature at depth was calculated using Eq. (2) in the uppermost layer up to the temperature T_1 at the bottom of the layer ($z = h_1$). The temperature in the second layer ($z > h_1$) was calculated using similar parabolic depth dependency:

$$T(z) = T_1 + (z - h_1)(q_1/K_2) - (z - h_1)^2 H_2/(2K_2) \quad (3)$$

Table 1
Thermal conductivities of different rocks (data from Eckstein and Simmons, 1978 and Maurath, 1989).

Rock type	Thermal conductivity (W/°C/m)	n	σ
Limestone	2.1	28	0.14
Dolomite	3.5	23	0.13
Chalk and Marl	1.3	16	0.22
Clay and Shales	1.2	6	0.17
Sandstone and Siltstone	2.1	40	0.35
Salt	3.2	24	0.34
Basalt	1.7	13	0.09
Upper crust basement	2.8	–	–
Lower crust (below 20 km depth)	2.5		

where K_2 and H_2 are the thermal conductivity and the radiogenic heat production of the second layer; the heat flux, q_1, at the interface between the first and the second layer is:

$$q_1 = q_s - h_1 H_1. \quad (4)$$

Similar procedure was applied to the temperature calculation in deeper layers. Temperature at 4 km depth is shown in Fig. 5. The contouring is based on the depth profile of the boreholes (black circles) and is linearly interpolated between the boreholes using the ANUDEM computer algorithm (Hutchinson, 1989).

Fig. 6 shows the temperature distribution calculated using the procedure described above (Eqs. (2)–(4)) on a cross-section along the Dead Sea Fault. The one dimensional solution serves as a good approximation, because the horizontal temperature gradient is at least five times smaller than the vertical temperature gradient. The surface heat flux shown as a curve at the top of the figure emphasizes the low heat flux at the Dead Sea as opposed to the relatively high heat flux at the Sea of Galilee and the Gulf of Eilat. Temperature contours of 300 °C and 350 °C are shown in bold black lines. Below these temperatures, deformation is expected to be brittle (Blanpied et al., 1995; Sholtz, 1998), and therefore this temperature range should mark the depth of the seismogenic zone. It is shown in Fig. 6 that there is

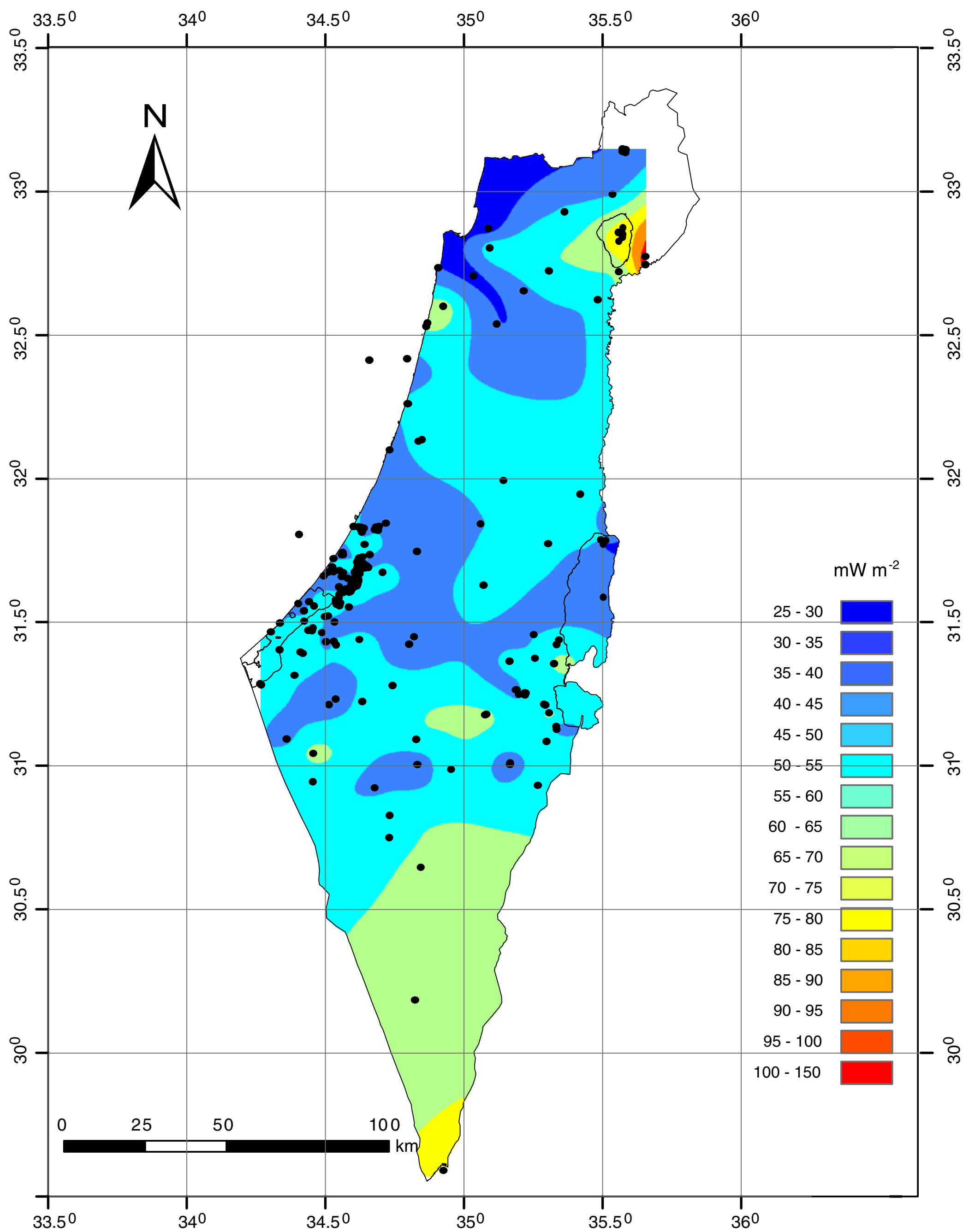

Fig. 4. Calculated geothermal heat flux in Israel from borehole temperature measurements. South east of the Sea of Galilee and in southern Israel the heat flux is relatively high. Black dots represent the boreholes used for the calculation and interpolation.

a good correlation between the temperature contours of 300 °C and 350 °C and the depth of the seismogenic zone as defined by earthquake locations. These are reported by the European-Mediterranean Seismological Centre catalog (2011) for the entire Dead Sea fault area, by Aldersons et al. (2003) and Shamir (2006) for the Dead Sea area, and by Navon (2011) for the Sea of Galilee area, respectively.

5. Discussion

The average geothermal heat flux throughout Israel is low (40–45 mW/m^2), compatible with the previous studies of the region (Ben-Avraham et al., 1978; Eckstein and Simmons, 1978). Such low heat flux is also consistent with the measurements at the Arabian Shield (Gettings and Showail, 1982). In southern Israel, the relatively high heat flux values are similar to the flux found by Förster et al. (2007, 2010) in this area, which probably represent the effects of the opening of the Red Sea but not the common heat flux in Israel.

At northern Israel, there is a thermal and heat flux anomaly southeast of the Sea of Galilee. This anomaly could be attributed to groundwater flow from depths along faults, which are common at this area. Alternatively, this could be related to crustal heating associated with the young magmatic activity in this area (activity ceased ~100,000 years ago; Roded, 2012).

Upper mantle (lithospheric) and lower crustal xenoliths, including peridotites, pyroxenites and mafic granulites, are found in Israeli and other basalts in the Arabian peninsula (Fig. 1). Thermobarometric calculations, based on mineral equilibrium, usually yield relatively high temperatures and steep geothermal gradients (Al-Mishwat and Nasir,

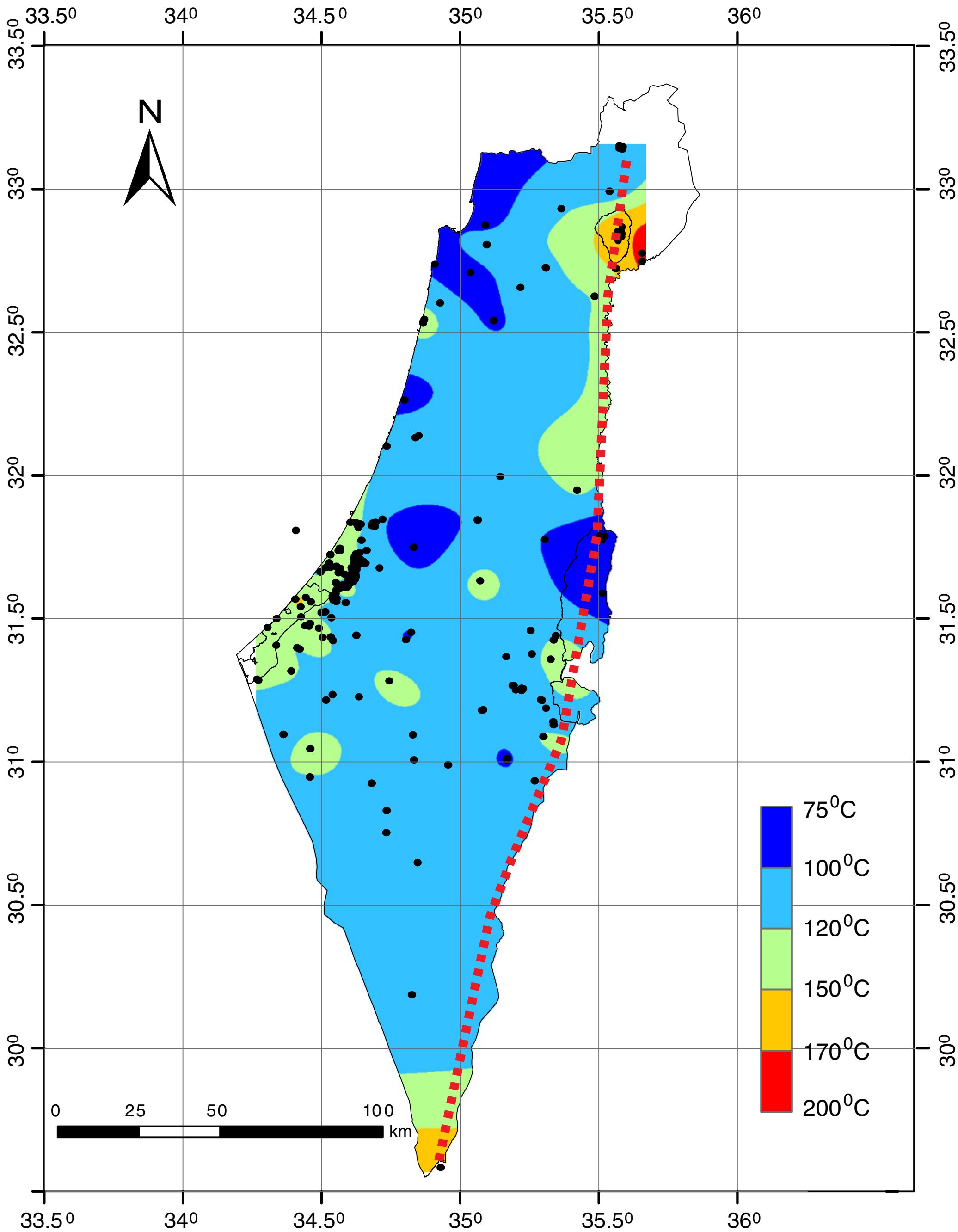

Fig. 5. Temperature distribution at 4 km depth. Black dots represent the boreholes used for the calculation and interpolation. The red dotted line represents the location of the cross-section showed in Fig. 6.

2004; Gazit, 2005; McGuire, 1988; McGuire and Bohannon, 1989; Nasir, 1992; Stein et al., 1993), e.g. 1,015 °C at 15 kbar. This implies a surface heat flux >80 mW/m^2, in prominent disagreement with the above. However, the measured high temperatures in xenoliths could as well be the result of local heating at depth by the ascending magmas (Stein et al., 1993; Weinstein et al., 2006) with no impact on regional heat flux. Moreover, several recent studies suggest that strain localization and development of necking instabilities may occur even in cold lithosphere due to very limited stretching (Benallal and Bigoni, 2004; Kaus and Podladchikov, 2006; Regenauer-Lieb and Yuen, 2004; Regenauer-Lieb et al., 2006; Rosenbaum et al., 2010; Weinberg et al., 2007). Accordingly, a limited extension of the cold Arabian shield could have led to the development of localized lithospheric necking and shear heating required for the high equilibrium temperature documented by the xenoliths. The hypothesis of necking instabilities and strain localization was not yet investigated in context of the regional volcanism.

Alternatively, Förster et al. (2010) suggested that the high P–T indicated by lower crustal xenoliths is a 'frozen-in' signal, which represents P–T conditions from the Pan-African, Late Proterozoic time (>600 Ma). This suggestion is compatible with the age of most xenoliths that is assumed to be Pan African, though age determination were hardly performed, and when done some younger ages were also documented (e.g., 300–400 Ma; Stein, 1987; Weinstein, 1998).

The temperature distribution along the Dead Sea Fault (Fig. 6) is in agreement with the depth of the seismic activity. The deep seismic activity at the Dead Sea, reported by Aldersons et al. (2003), Shamir

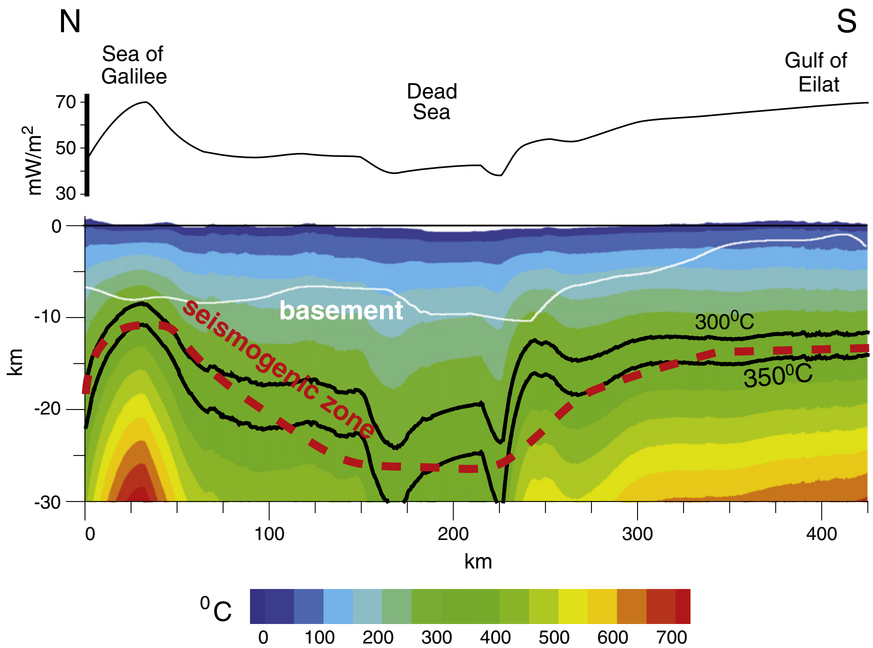

Fig. 6. Temperature distribution on a cross-section along the Dead Sea Fault (see Fig. 5 for location). The surface heat flux (top) served as input into this calculation. The basement is marked by a solid white line. The seismogenic zone (red dashed line) is based on data from European-Mediterranean Seismological Centre catalog (2011) for the entire area, data from Aldersons et al. (2003) and Shamir (2006) for the Dead Sea area, and data from Navon (2011) for the Sea of Galilee area.

(2006), and Braeuer et al. (2010) suggests that the lower crust is cold and brittle. This is consistent with the low heat flow of 40 mW/m^2. This situation is different from that of the San Andreas Fault, where the majority of the seismic activity takes place in the upper crust, shallower than ~15 km depth (e.g., Magistrale, 2002; Rolandone et al., 2004). The slip rate along the San Andreas Fault is several times higher than that along the Dead Sea fault. Hence, one might expect a shallower seismogenic zone in Israel. It is probably the difference between the heat fluxes, 60–80 mW/m^2 in California (e.g., Blackwell and Richards, 2004a,b) and ~40 mW/m^2 in the Dead Sea, that is responsible for the anomalously deep seismicity at the Dead Sea area. A relatively shallow seismogenic zone, with maximum depths of ~10 km in the Gulf of Eilat and ~12 km in the Sea of Galilee (Fig. 6) is compatible with the elevated heat flux, up to ~70 mW/m^2. In these parts of the Dead Sea Fault both heat flux and the depth of the seismogenic zone is similar to the values reported for California.

Ben-Avraham and Schubert (2006) proposed a conceptual model of a "drop down" mechanism for the formation of the Dead Sea basin, as an alternative to the classic pull-apart approach. According to their suggestion, propagating faults isolated a block of lithosphere that dropped into the mantle. Ben-Avraham et al. (2010) provided a quantitative description of this process by 3-D numerical simulations in a model with a seismogenic crust governed by a continuum damage rheology. Their modeling suggests that a heavy magmatic body, formed in the crust or upper mantle during previous stages of regional magmatism, started dropping down into the upper mantle when the strike-slip faults were created. The isostatically non-compensated heavy body detached from the surrounding lithosphere sunk and pulled down the crustal block above it, providing the main driving mechanism for the formation of the Dead Sea basin. Numerical simulations indicate that the resulting basin is rhomb-shaped, which grows by the addition of distinct segments to its edges and that the fault geometry mimics the pull-apart rhomb-shaped structure. Nevertheless, the mechanism of the basin formation is very different. The proposed mechanism appears to account for the observed low heat flow and deep seismicity in the Dead Sea.

6. Conclusions

Re-examination of temperature data confirms that the common geothermal heat flux throughout Israel is low (40–45 mW/m^2). The heat flux is higher in southern Israel as a result of the opening of the Red Sea. In northeastern Israel, the relatively high heat flux is attributed to groundwater flow or to the young magmatic activity (~100,000 years) that is common in this area. The steeper geothermal gradients implied by data from xenoliths could be the result of local heating either by the magmatic activity or by lithospheric necking and shear heating. The temperature gradient at the Dead Sea basin is relatively low, resulting in a relatively deep seismogenic zone (with a maximum depth of 15 km), in agreement with estimates based on earthquake depths.

Acknowledgments

We would like to thank the editor S. Cloetingh for his constructive remarks. We appreciate the thorough evaluations of our manuscript by Dr. Gideon Rosenbaum and two additional anonymous reviewers. This project was funded by Ormat Systems, Inc. V. Lyakhovsky acknowledges support from the Israel Science Foundation (grant ISF 753/08).

References

Aldersons, F., Ben-Avraham, Z., Hofstetter, A., Kissling, E., Al-Yazjeen, T., 2003. Lower-crustal strength under the Dead Sea basin from local earthquake data and rheological modeling. Earth and Planetary Science Letters 214, 129–142.

Al-Mishwat, A.T., Nasir, S.J., 2004. Composition of the lower crust of the Arabian Plate: a xenolith perspective. Lithos 72, 45–72.

Al-Zoubi, A., ten Brink, U., 2002. Lower crustal flow and the role of shear in basin subsidence: an example from the Dead Sea basin. Earth and Planetary Science Letters 199, 67–79.

Bein, A., Feinstein, S., 1988. Late Cenozoic thermal gradients in the Dead Sea transform system basins. Journal of Petroleum Geology 11, 185–192.

Benallal, A., Bigoni, D., 2004. Effects of temperature and thermo-mechanical couplings on material instabilities and strain localization of inelastic materials. Journal of Mechanical Physics Solar 52, 725–753. http://dx.doi.org/10.1016/S0022-5096(03)00118-2.

Ben-Avraham, Z., Schubert, G., 2006. Deep "Drop Down" basin in the southern Dead Sea. Earth and Planetary Science Letters 251, 254–263.

Ben-Avraham, Z., Hänel, R., Villinger, H., 1978. Heat flow through the Dead Sea rift. Marine Geology 28, 253–269.

Ben-Avraham, Z., Lyakhovsky, V., Schubert, G., 2010. Drop-down formation of deep basins along the Dead Sea and other strike-slip fault systems. Geophysical Journal International 181, 185–197.

Blackwell, D. D. Richards, M., 2004a. Geothermal Map of North America. Amer. Assoc. Petroleum Geologists, Tulsa, Oklahoma, 1 sheet, scale 1:6,500,000.

Blackwell, D.D., Richards, M., 2004a. Calibration of the AAPG Geothermal Survey of North America BHT Data Base. AAPG Annual Meeting, Dallas, Tx, paper 87616.

Blackwell, D.D., Negraru, P.T., Richards, M., 2007. Assessment of the Enhanced Geothermal System Resource Base of the United States. Natural Resources Research 15. http://dx.doi.org/10.1007/s11053-007-9028-7.

Blanpied, M.L., Lockner, D.A., Byerlee, J.D., 1995. Frictional slip of granite at hydrothermal conditions. Journal of Geophysical Research 100, 13,045–13,064.

Braeuer, B., Asch, G., Hofsetter, R., Haberland, Ch., Jaser, D., El-Kelani, R., Weber, M., 2010. Microseismicity distribution in the southern Dead Sea basin and its implications on the structure of the basin. Geophysical Journal International. http://dx.doi.org/10.1111/j.1365-246X.2011.05318.x.

Davies, J.H., Davies, D.R., 2010. Earth's surface heat flux. Solid Earth 1, 5–24.

Dubertret, L., 1954. Carte Geologique Beyrouth 1:200,000.

Eckstein, Y., 1976. The measurement and interpretation of terrestrial heat flow in Israel. Israel Geological Survey Reports on Hydrology 3, 76.

Eckstein, Y., Simmons, G., 1978. Measurement and interpretation of terrestrial heat flow in Israel. Geothermics 6, 117–142.

Eckstein, Y., Maurath, G., 1995. Terrestrial heat flow density and geothermal regime in Israel. In: Gupta, M.L., Yamano, M. (Eds.), Terrestrial Heat Flow and Geothermal Energy in Asia. Oxford & IBH, New Delhi, pp. 1–21.

European-Mediterranean Seismological Centre catalog, 2011. http://www.emsc-csem.org/.

Förster, A., 2001. Analysis of borehole temperature data in the Northern German Basin: continuous logs versus bottom-hole temperatures. Petroleum Geosciences 7, 241–254.

Förster, A., Förster, H.-J., Masarweh, R., Masri, A., Tarawneh, K., DESERT Group, 2007. The surface heat flow of the Arabian Shield in Jordan. Journal of Asian Earth Sciences 30, 271–284.

Förster, H.-J., Förster, A., Oberhänsli, R., Stromeyer, D., 2010. Lithospheric composition and thermal structure of the Arabian Shield in Jordan. Tectonophysics 481, 29–37.

Galanis, S.P., Sass, J.H., Munroe, R.J., Abu-Ajamieh, M., 1986. Heat flow at Zerqa Ma'in and Zara and a geothermal reconnaissance of Jordan. U.S.Geological Survey Open-File Report, 86–631, p. 110.

Garfunkel, Z., 1988. The pre-Quaternary geology of Israel. In: Yom-Tov, Y., Tchernov, E. (Eds.), The Zoogeography of Israel. Jungk Publishers, Dordrecht, pp. 7–34.

Gazit, O., 2005. Mafic granulite xenoliths from Qarnei Hittin and the evolution of the lower crust beneath northern Israel. (In Hebrew; Engl. Abstr.) Israel Geological Survey Reports (GSI/11/05, 67 pp.).

Gettings, M.E., Showail, A., 1982. Heat-flow measurements at shot points along the 1978 Saudi Arabian deep-refraction line, Part I: results of measurements. Open File Report USGS-OF-02-39. Saudi Arabia Deputy Min. for Mineral Res (98 pp.).

Ginzburg, A., Gvirtzman, G., 1979. Changes in the crust and in the sedimentary cover across the transition from the Arabian Platform to the Mediterranean Basin: evidence from seismic refraction and sedimentary studies in Israel and in Sinai. Sedimentary Geology 23, 19–36.

Gvirtzman, H., Garven, G., Gvirtzman, G., 1997. Thermal anomalies associated with forced and free ground-water convection in the Dead Sea rift valley. Geological Society of American Bulletin 109, 1167–1176.

Harrison, W.E., Luza, K.V., Prater, M.L., Chueng, P.K., 1983. Geothermal resource assessment of Oklahoma. Special Publication 83–1. Geological Survey, Okla.

Hutchinson, M.F., 1989. A new procedure for gridding elevation and stream line data with automatic removal of spurious pits. Journal of Hydrology 106, 211–232.

Jaupart, C., Mareschal, J.C., 2011. Heat generation and transport in the Earth. Cambridge University Press.

Kaus, B.J.P., Podladchikov, Y.Y., 2006. Initiation of localized shear zones in viscoelstoplastic rocks. Journal of Geophysical Research 111, B04412. http://dx.doi.org/10.1029/2005JB003652.

Kehle, R.O., Schoeppel, R.J., Deford, R.K., 1970. The AAPG geothermal survey of North America. Geothermics 2, 358–367. http://dx.doi.org/10.1016/0375-6505(70)90034-9.

Kovach, R.L., Andreasen, G.E., Gettings, M.E., El-Kaysi, K., 1990. Geophysical investigations in Jordan. Tectonophysics 180, 61–69.

Levitte, D., Maurath, G., Eckstein, Y., 1984. Terrestrial heat flow in a 3.5 km deep borehole in the Jordan-Dead Sea rift valley. Geological Society of America Abstracts with Programs 16, 575.

Magistrale, H., 2002. Relative contributions of crustal temperature and composition to controlling the depths of earthquakes in southern California. Geophysical Research Letters 29 (10), 1447.

Maurath, G., 1989. Thermal constraints on tectonic processes along the Jordan-Dead Sea Transform. Ph.D. dissertation submitted to Kent State University.

McGuire, A.V., 1988. Petrology of mantle xenoliths from Harrat al Kishb: the mantle beneath western Saudi Arabia. Journal of Petrology 29, 73–92.

McGuire, A.V., Bohannon, R.G., 1989. Timing of mantle upwelling: evidence for a passive origin of the Red Sea rift. Journal of Geophysical Research 94B, 1677–1682.

Mor, D., 1993. A time-table for the Levant volcanic province, according to K–Ar dating in the Golan Heights. Israel Journal African Earth Science 16 (3), 223–234.

Nasir, S., 1992. The lithosphere beneath the northwestern part of the Arabian plate (Jordan): evidence from xenoliths and geophysics. Tectonophysics 201, 357–370.

Navon, H., 2011. Microseismic characterization of Lake Kinneret basin, M.Sc. thesis. Tel-Aviv University.

Petrunin, A., Sobolev, S.V., 2006. What controls thickness of sediments and lithospheric deformation at a pull-apart basin? Geology 34, 389–392.

Ranalli, G., 1995. Rheology of the Earth, 2nd ed. Chapman & Hall, London, p. 436.

Ranalli, G., Rybach, L., 2005. Heat flow, heat transfer and lithosphere rheology in geothermal areas: features and examples. Journal of Volcanology and Geothermal Research 148, 3–19.

Regenauer-Lieb, K., Yuen, D., 2004. Positive feedback of interacting ductile faults from coupling of equation of state, rheology and thermal-mechanics. Physics of the Earth and Planetary Interiors 142, 113–135. http://dx.doi.org/10.1016/j.pepi.2004.01.003.

Regenauer-Lieb, K., Weinberg, R.F., Rosenbaum, G., 2006. The effect of energy feedback on continental strength. Narure 442, 67–70.

Roded, R., 2012. Basal heat flow and hydrothermal regime at the Golan-Ajloun hydrological Basins. M.Sc. thesis. Ben-Gurion University.

Rolandone, F., Bürgmann, R., Nadeau, R.M., 2004. The evolution of the seismic–aseismic transition during the earthquake cycle: constraints from the time-dependent depth distribution of aftershocks. Geophysical Research Letters 32. http://dx.doi.org/10.1029/2004GL021379.

Rosenbaum, G., Regenauer-Lieb, K., Weinberg, R.F., 2010. Interaction between mantle and crustal detachments: a nonlinear system controlling lithospheric extension. Journal of Geophysical Research 115, B11412. http://dx.doi.org/10.1029/2009JB006696.

Rybakov, M., Segev, A., 2004. Top of the crystalline basement in the Levant. Geochemistry, Geophysics, Geosystems 5. http://dx.doi.org/10.1029/2004GC000690.

Segev, A., Rybakov, M., Lyakhovsky, V., Hofstetter, A., Tibor, G., Goldshmidt, V., Ben Avraham, Z., 2006. The structure, isostasy and gravity field of the Levant continental margin and the southeast Mediterranean area. Tectonophysics 425, 137–157.

Shaanan, U., Porat, N., Navon, O., Weinberger, R., Calvert, A., Weinstein, Y., 2010. OSL dating of a Pleistocene maar: Birket Ram, the Golan Heights. Journal of Volcanology and Geothermal Research 201, 397–403. http://dx.doi.org/10.1016/j.jvolgeores.2010.06.007.

Shalev, E., Lyakhovsky, V., Yechieli, Y., 2007. Is convective heat transport significant at the Dead Sea Basin? Geofluids 7, 292–300.

Shalev, E., Levitte, D., Gabay, R., Zemach, E., 2008. Assessment of geothermal resources in Israel. Israel Geological Survey Reports (GSI/29/2008, 26 pp.).

Shaliv, G., 1991. Stages in the tectonic and volcanic history of the Neogene basin in the Lower Galilee and the Valleys. Israel Geological Survey Reports (GSI/11/91, 94 pp. (in Hebrew)).

Shamir, G., 2006. The active structure of the Dead Sea Depression. In: Enzel, Y., Agnon, A., Stein, M. (Eds.), New frontiers in Dead Sea paleoenvironmental researchGeological Society of America, Special Paper 401, 15–32.

Sholtz, C.H., 1998. Earthquakes and friction laws. Nature 391, 37–42.

Smit, J., Brun, J.-P., Fort, X., Cloetingh, S., Ben-Avraham, Z., 2008a. Salt tectonics in pullapart basins with application to the Dead Sea basin. Tectonophysics 449, 1–16.

Smit, J., Brun, J.-P., Cloetingh, S., Ben-Avraham, Z., 2008b. Pull-apart basin formation and development in narrow transform zones with application to the Dead Sea Basin. Tectonics 27, TC6018. http://dx.doi.org/10.1029/2007TC002119.

Smit, J., Brun, J.-P., Cloetingh, S., Ben-Avraham, Z., 2010. The rift-like structure and asymmetry of the Dead Sea Fault. Earth and Planetary Science Letters 290, 74–82.

Sobolev, S.V., Petrunin, A., Garfunkel, Z., Babeyko, A.Y., 2005. Thermo-mechanical model of the Dead Sea Transform. Earth and Planetary Science Letters 238, 78–95.

Stein, M., 1987. Ultra-basic xenoliths in Cenozoic and Mesozoic volcanic rocks in Israel. Ph.D. thesis, Hebrew University, Jerusalem.

Stein, M., Garfunkel, Z., Jagoutz, E., 1993. Chronothermometry of peridotitic and pyroxenitic xenoliths: implications for the thermal evolution of the Arabian lithosphere. Geochimica et Cosmochimica Acta 57, 1325–1337.

Tester, J.W., Anderson, B.J., Batchelor, A.S., Blackwell, D.D., DiPippo, R., Drake, E.M., Garnish, J., Livesay, B., Moore, M.C., Nichols, K., Petty, S., Toksöz, M.N., Veatch Jr., R.W., 2006. The Future of Geothermal Energy: impact of Enhanced Geothermal Systems (EGS) on the United States in the 21st Century. Massachusetts Institute of Technology, Cambridge, MA, USA, available at http://geothermal.inel.gov and http://www1.eere.energy.gov/geothermal/egs_technology.html.

Truesdell, A., Duffield, W., Abu Ajamieh, M., 1983. Origin and heat source of thermal waters at Zarqa Ma'in and Zara, Jordan: extended abstracts of 4th Intl. Symposium on Water-Rock Interactions, Misasa, Japan, Aug. 29-Sep. 3, pp. 508–811.

Weinberg, R.F., Regenauer-Lieb, K., Rosenbaum, G., 2007. Mantle detachment and the break-up of cold continental crust. Geology 35 (11), 1035–1038. http://dx.doi.org/10.1130/G23918A.1.

Weinstein, Y., 1998. Mechanisms of generation of intra-continental alkali-basalts in northeastern Israel. Ph.D. thesis, Hebrew University, Jerusalem.

Weinstein, Y., Navon, O., Altherr, R., Stein, M., 2006. The role of fluids and of lithospheric heterogeneity in the generation of alkali basaltic suites from northwestern Arabia. Journal of Petrology 47, 1017–1050.

Weinstein, Y., Weinberger, R., Shaanan, U., 2009. Magma and water — explosive and collapse structures in the northern Golan. Israel Geol. Soc. Meeting, Kfar Blum.